

## Feasibility of automated early postnatal sleep staging in extremely and very preterm neonates using dual-channel EEG



Xiaowan Wang<sup>a</sup>, Anne Bik<sup>a</sup>, Eline R. de Groot<sup>a</sup>, Maria Luisa Tataranno<sup>a,b</sup>, Manon J.N.L. Benders<sup>a,b</sup>, Jeroen Dudink<sup>a,b,\*</sup>

<sup>a</sup> Department of Neonatology, Wilhelmina Children's Hospital, University Medical Center Utrecht, Utrecht, The Netherlands

<sup>b</sup> Brain Center Rudolf Magnus, University Medical Center Utrecht, Utrecht, The Netherlands

### HIGHLIGHTS

- Dual-channel quantitative EEG metrics are useful to distinguish between sleep-wake states of preterm neonates in the first postnatal hours.
- Combining different qEEG metrics helps develop a sleep-wake state classifier robust against rapid maturational changes in the preterm period.
- The complexity features showed the best sleep staging capability and greatest robustness among several quantitative EEG metrics.

### ARTICLE INFO

#### Article history:

Accepted 30 November 2022

Available online 7 December 2022

#### Keywords:

Preterm  
Early postnatal period  
Preterm sleep  
Automated sleep staging  
Quantitative EEG  
Complexity analysis

### ABSTRACT

**Objective:** To investigate the feasibility of automated sleep staging based on quantitative analysis of dual-channel electroencephalography (EEG) for extremely and very preterm infants during their first postnatal days.

**Methods:** We enrolled 17 preterm neonates born between 25 and 30 weeks of gestational age. Three-hour behavioral sleep observations and simultaneous dual-channel EEG monitoring were conducted for each infant within their first 72 hours after birth. Four kinds of representative and complementary quantitative EEG (qEEG) metrics (i.e., bursting, synchrony, spectral power, and complexity) were calculated and compared between active sleep, quiet sleep, and wakefulness. All analyses were performed in offline mode.

**Results:** In separate comparison analyses, significant differences between sleep-wake states were found for bursting, spectral power and complexity features. The automated sleep-wake state classifier based on the combination of all qEEG features achieved a macro-averaged area under the curve of receiver operating characteristic of 74.8%. The complexity features contributed the most to sleep-wake state classification.

**Conclusions:** It is feasible to distinguish between sleep-wake states within the first 72 postnatal hours for extremely and very preterm infants using qEEG metrics.

**Significance:** Our findings offer the possibility of starting personalized care dependent on preterm infants' sleep-wake states directly after birth, potentially yielding long-run benefits for their developmental outcomes.

© 2022 International Federation of Clinical Neurophysiology. Published by Elsevier B.V. This is an open access article under the CC BY license (<http://creativecommons.org/licenses/by/4.0/>).

**Abbreviations:** EEG, electroencephalography; aEEG, amplitude-integrated EEG; qEEG, quantitative EEG; AS, active sleep; QS, quiet sleep; NICU, neonatal intensive care unit; MSE, multiscale entropy.

\* Corresponding author at: Department of Neonatology, Wilhelmina Children's Hospital, University Medical Center Utrecht, KH.03.419.1, Utrecht, The Netherlands.

E-mail address: [j.dudink@umcutrecht.nl](mailto:j.dudink@umcutrecht.nl) (J. Dudink).

<https://doi.org/10.1016/j.clinph.2022.11.018>

1388–2457/© 2022 International Federation of Clinical Neurophysiology. Published by Elsevier B.V. This is an open access article under the CC BY license (<http://creativecommons.org/licenses/by/4.0/>).

## 1. Introduction

Preterm birth, especially very early prematurity (<30 weeks of gestational age, wks GA), exposes the newborn brain to an extra-uterine environment at a time when critical developmental processes emerge (Humberg et al., 2020; Pierrat et al., 2021; Tau and Peterson, 2010; Volpe, 2019). Evidence has shown that neonatal sleep-wake organization has long-term impacts on later life

(Anders et al., 1985; Bennet et al., 2018). For establishing a healthy sleep pattern, it is important to personalize care plans according to the infant's sleep/wake cycle, and to integrate caregiving activities that promote sleep into the routine clinical care in the neonatal intensive care unit (NICU) (Als and McNulty, 2011; Altimier and Phillips, 2016). Hence, an appropriate sleep assessment tool is urgently needed to help caregivers to identify the infant's sleep-wake states in the NICU.

There are primarily three distinct sleep-wake states during the preterm period: active sleep (AS), quiet sleep (QS), and wakefulness (W) (Brazelton and Nugent, 1995; Georgoulas et al., 2021; Prechtl, 1974). Between the three states, transitional periods or undifferentiated states, such as drowsiness and intermediate sleep (IS), are also commonly seen in premature infants. Traditionally, the assessment of preterm sleep-wake states in the NICU is performed by sleep specialists based on direct behavioral observation and/or visual evaluation of multiple-parametric polysomnography (PSG) recordings, among which electroencephalography (EEG) signals play a pivotal role (Grigg-Damberger et al., 2007; Werth et al., 2017). However, the visual sleep scoring techniques suffer from several drawbacks, such as the tedious nature of manual labeling work, proneness to subjective bias, prohibitive cost, and extensive training and experience requirements. It is, therefore, necessary to develop a new approach for automated sleep staging in preterm infants admitted to the NICU.

Quantitative EEG (qEEG) analysis has exhibited promising potential for developing a fully automated neonatal sleep staging system (Dereymaeker, Pillay, Vervisch, De Vos, et al., 2017). Using mathematical and statistical algorithms, the qEEG analysis extracts numerical parameters from raw EEG signals (Tong and Thankor, 2009). The qEEG parameters can be utilized not only to depict key clinical features of preterm EEG, such as discontinuity, but also to uncover hidden attributes from EEG signals, such as spectral properties (Hrachovy and Mizrahi, 2015; Watanabe et al., 1999). Compared to complicated black-box models, a qEEG-based automated sleep classification model is explainable and can assist clinicians in making informed decisions in the NICU (Petch et al., 2021).

So far, however, the role of qEEG in sleep staging is less well-studied in premature infants born before 30 wks GA (i.e., extremely-to-very preterm infants) despite the improved survival rates of this population. Several recent studies have attempted to, at least partially, cover this age group (De Wel et al., 2017; Dereymaeker, Pillay, Vervisch, Van Huffel, et al., 2017; Koolen et al., 2017). Still, these findings might have been affected by using non-validated visual sleep labeling methods for this population (Bik et al., 2022). Moreover, these studies focused only on QS and non-QS state classification regardless of the important role of AS in early brain development (Del Rio-Bermudez and Blumberg, 2018; Knoop et al., 2021).

Furthermore, extremely and very preterm infants are particularly susceptible to brain impairment during the first postnatal days (Benders et al., 2015; Rice and Jr, 2000). Given the different roles of alternating sleeping and waking states in early brain development (Knoop et al., 2021), it is necessary to start providing appropriate caregiving activities contingent on the infant's state as early as possible. However, it remains unknown whether the qEEG measures would still be a valuable tool for determining different sleep-wake states in newly born preterm infants. Existing preterm sleep-qEEG research has focused on multichannel EEG montages that are difficult to apply to preterm newborns due to their tiny heads and vulnerable skin (De Wel et al., 2017; Dereymaeker, Pillay, Vervisch, Van Huffel, et al., 2017; Koolen et al., 2017; Paul et al., 2003). In contrast, dual-channel amplitude-integrated EEG (aEEG) with access to raw EEG traces is a simplified technique readily available in many NICUs world-

wide for bedside monitoring of preterm cerebral function (Tao and Mathur, 2010). Due to its less invasive nature, the (a)EEG monitoring can be initiated shortly after birth, providing a unique window of opportunity to identify the preterm newborn's earliest sleep-wake states.

In this light, the current study targets the least studied preterm age group (<30 wks GA) and aims to evaluate the ability of qEEG characteristics in distinguishing between sleep-wake states during their first days after birth. Sleep annotation was performed by using a recently published behavioral sleep scoring system from our group, which is, to our knowledge, the first system validated for extremely and very preterm infants (de Groot et al., 2022). To provide easily interpretable results, we extracted several representative qEEG measures, including bursting, synchrony, spectral power, and complexity, from dual-channel EEG signals and provided a statistical description of how each separate qEEG feature is distributed across the states of AS, QS, and W. We also aim to identify which specific qEEG parameters are more powerful in discriminating between sleep-wake states.

## 2. Methods

### 2.1. Patients

The current study enrolled 17 infants born extremely or very preterm (10 males; mean wks GA = 27.69, standard deviation (SD) = 1.16, range 25.14 – 29.43 wks GA) and admitted to the NICU of the Wilhelmina Children's Hospital (Utrecht, The Netherlands). All enrolled infants received continuous dual-channel EEG monitoring combined with three-hour visual sleep observation during their first three days after birth. Exclusion criteria were: congenital malformations, seizures, overt brain injury on cerebral ultrasound (e.g., intraventricular hemorrhage grade III-IV), and mother's use of recreational drugs during pregnancy. The study protocol (No. 21-066-C) was reviewed by the Medical Research Ethics Committee (MREC / METC) of the University Medical Center Utrecht, who confirmed that the Medical Research Involving Human Subjects Act (WMO) does not apply to this study. Written informed consent was obtained from parents before enrollment. All data were anonymized prior to analysis.

### 2.2. Visual sleep observation

For each patient, three consecutive hours of bedside sleep observation were carried out between 9 am and 7 pm at the NICU within the first three days after birth. Sleep-wake states were manually annotated by two independent observers (AB and EG) using an in-house behavioral sleep scoring system developed and validated for extremely and very preterm infants, called *BeSSPI* (de Groot et al., 2022). The inter-rater reliability was assessed by Fleiss' Kappa, yielding a  $\kappa$  value of 0.79. Four behavioral states, AS, IS, QS and W, were assigned to discrete one-minute epochs based on behavioral measurements, including eyes, vocalizations, facial and body movements, and vital physiologic parameters, including heart and respiratory rate. The vital signs were measured using a mobile bedside patient monitor (IntelliVue MP70, Philips Healthcare, Best, The Netherlands). A smoothing procedure was applied to the observational sleep annotations to increase scoring accuracy by accounting for temporal context information. Details of the sleep observation method can be found in de Groot et al. (2022). The sleep observation could be interrupted by several caretaking events and these interruption epochs were treated as missing values. In the *BeSSPI*, the state of IS is defined as a temporary transitional period either between sleep states (i.e., AS and QS), or between sleep and wake (e.g., AS and W). As a heterogeneous state,

it blends characteristics of different behavioral states together and lacks typical EEG features (Tsuchida et al., 2013). To avoid bias, the IS states were thus excluded from subsequent statistical analysis.

### 2.3. Dual-channel (a)EEG monitoring

Dual-channel (a)EEG monitoring during sleep observation was performed using the BrainZ monitor (Natus Medical Inc., Seattle, WA). Raw EEG signals were recorded at a sampling rate of 256 Hz. Four needle electrodes were placed subcutaneously over the frontal and parietal lobes (F3, F4, P3, P4) according to the International 10–20 system (Jasper, 1958; Shellhaas et al., 2011). In addition, a center electrode was used as reference. A dual-channel bipolar montage derived from the four active electrodes (left: F3–P3, right: F4–P4) was used for subsequent quantitative EEG analysis.

### 2.4. Quantitative EEG metrics

Four types of qEEG metrics were extracted from raw EEG data: 1) bursting, 2) synchrony, 3) spectral power, and 4) complexity. These metrics were selected because of their great potential to capture neonatal sleep cycling and their close associations with neonatal brain functional development (De Wel et al., 2021; O'Toole and Boylan, 2019). Moreover, different types of qEEG features can provide complementary information and combining them might help improve automated sleep classification performance.

Intermittent bursting activity, also known as spontaneous activity transients (SATs), is a dominant EEG feature in early stages of preterm infancy (Vanhatalo and Kaila, 2006). We detected SATs using an automated detection algorithm as presented in Palmu et al. (2010). Three indices of bursting features were calculated: 1) number of SATs per minute (SAT rate), 2) interval duration of the inter-SAT interval (ISI), and 3) percentage of inter-SAT duration per minute (ISP). These features measure the degree of discontinuity of EEG activity. Lower SAT rate, higher ISP, and longer ISI are correlated with a larger amount of discontinuity in EEG tracing (Louis et al., 2016).

The degree of interhemispheric synchrony is estimated by activation synchrony index (ASI), which quantifies the temporal coincidence of bursting activity in left and right hemispheres (Koolen et al., 2014; Räsänen et al., 2013). A higher ASI value indicates profusion of coincidences, while a lack of coincidences results in a lower ASI value.

Spectral power analysis was used to quantify spectral characteristics of EEG. Absolute and relative spectral power of four different frequency bands were computed: delta ( $\delta$ ): 0.5–3 Hz, theta ( $\theta$ ): 3–8 Hz, alpha ( $\alpha$ ): 8–15 Hz, beta ( $\beta$ ): 15–30 Hz (O'Toole et al., 2016; Tokariev et al., 2012). Absolute power describes the average power of a specific frequency band and relative power is expressed as the ratio of the absolute power to total power of all four bands.

Multiscale entropy (MSE), as a complementary measure of spectral power, characterizes the dynamic complexity of EEG signals by quantifying sample entropy over multiple temporal scales (Costa et al., 2002, 2005). The range of the time scale factor  $\tau$  is set as 1–20. The MSE curve was generated by plotting the sample entropy as a function of the scale factor. Four features were extracted from the MSE curve: 1) the area under the curve, 2) the maximum value of the curve, 3) the average slope of fine scales ( $\tau$ : 1–5), and 4) the average slope of coarse scales ( $\tau$ : 6–20). The complexity index was defined as the area under the MSE curve. An increased complexity index suggests more unpredictable dynamics of the EEG time sequence, while a reduced value repre-

sents more repetitive EEG patterns (Courtiol et al., 2016; De Wel et al., 2017; Kosciessa et al., 2020).

Bursting analyses were performed using an in-house developed software SignalBase (version 10.6.4.0; University Medical Center Utrecht, Utrecht, The Netherlands). The rest of the qEEG analyses were conducted with in-house developed Matlab scripts (MathWorks Inc., Natick, MA, USA). To improve data quality, artifact correction and band-pass filtering (0.5–10 Hz for bursting features, 0.5–30 Hz for the other features) procedures were performed before feature extraction. The qEEG features were extracted from a short-duration window of 60 seconds and summarized across channels using the median value.

### 2.5. Statistical analysis

#### 2.5.1. Quantitative EEG feature distribution across sleep-wake states

For each qEEG feature a generalized linear mixed model (GLMM) with Wald Chi-square test was employed to detect statistically significant differences among different sleep-wake states. Because each patient occupies multiple epochs of sleep observation, the dependencies in the data were taken into account. Specifically, the qEEG feature was treated as dependent variable, sleep-wake state as a fixed effect, and patient identifier as a random effect in each GLMM. Considering that some of the features were not normally distributed, the distribution information of each qEEG feature was considered in the GLMM analysis. We used the Akaike information criterion (AIC) to choose an appropriate distribution to best fit each feature from normal, gamma, and log-normal distributions. Post-hoc multiple comparison procedures were conducted to identify differences of the qEEG features between each pair of the sleep states. The *P*-values were obtained by *T*-tests or *Z*-tests, as applicable.

Given the week-by-week developmental changes occurring during the newborn period (O'Toole et al., 2019; Stevenson et al., 2020), we further examined if differences exist between extremely preterm (EP, < 28 wks GA) and very preterm (VP, 28–30 wks GA) subgroups. The interaction effect of age  $\times$  sleep-wake state was also examined by using GLMM analysis with post-hoc testing, in which age was added as a fixed-effect factor. For all statistical analyses, the significance threshold was set at  $P < 0.05$ . Holm's procedure was used to adjust for multiple comparisons in post-hoc analyses. The GLMM analyses were performed using R (version 4.0.5) within R studio (version 1.4.1106).

#### 2.5.2. Automated sleep-wake state classification

Furthermore, we evaluated the role of the qEEG features in automated sleep-wake state classification. A multinomial logistic regression (MLR) model was built to automatically classify sleep-wake states into AS, QS, or W, using all of the qEEG features as predictors. The classification performance was measured by metrics of accuracy and macro-averaged area under the receiver operating characteristic curve (AUC of ROC) through a stratified 10-fold cross-validation procedure repeated 20 times. The statistical significance of each performance metric was assessed with a permutation test by shuffling the class labels 1000 times. To further test the effect of age, we also modeled a MLR classifier for EP and VP infants, respectively. The MLR classification analysis was implemented by using scikit-learn (version 0.23.2) within Python 3.8.5.

As the focus of the current study was not on designing a bedside or online implementation architecture, the whole analysis procedure (including all quantitative EEG analyses and statistical analysis) was executed offline on a personal computer with Intel Xeon W-2133 (3.60 GHz) processors.

### 3. Results

#### 3.1. Demographics and sleep characteristics

Demographic, behavioral, and clinical characteristics of all patients are detailed in Table 1 and Supplementary Table S1. A total of 2803 minutes of annotated sleep-wake data were collected, of which 1435 minutes were labeled as AS (51.2 %), 311 minutes as IS (11.1 %), 961 minutes as QS (34.3 %), and 96 minutes as W (3.4 %).

#### 3.2. Quantitative EEG features during different sleep states

As shown in Table 2, all qEEG features, except for ASI, differed significantly between sleep-wake states. Results of the post-hoc

**Table 1**  
Patient characteristics (n = 17).

Characteristics	All	EP	VP
Gender [M/F]	10/7	5/5	5/2
GA [weeks]	27.7 (1.16)	26.9 (0.81)	28.8 (0.56)
PMA at observation [weeks]	28.1 (1.20)	27.3 (0.83)	29.2 (0.55)
Birth weight [grams]	1130 (203)	1055 (156)	1239 (213)
Apgar score median			
1 min	6 (5, 8)	6 (4, 8)	7 (6, 8)
5 min	8 (7, 9)	8 (6, 8)	8 (8, 10)
10 min	9 (8, 9)	9 (8, 9)	9 (9, 10)
Observed sleep/wake states [minutes]			
AS	1435 (51.2 %)	895 (54.3 %)	540 (46.8 %)
IS	311 (11.1 %)	176 (10.7 %)	135 (11.7 %)
QS	961 (34.3 %)	531 (32.2 %)	430 (37.3 %)
W	96 (3.4 %)	47 (2.9 %)	49 (4.2 %)

Means were reported with their standard deviation in parentheses. Median Apgar scores were presented with interquartile range (quartile 1, quartile 3) in parentheses. Minutes of each observed sleep-wake state were presented with percentages relative to total observation time in parentheses. M = male; F = female; GA = gestational age; EP = extremely preterm; VP = very preterm; PMA = postmen-

**Table 2**  
Quantitative EEG measures across different sleep-wake states.

Feature type	Feature	Sleep states			Wald $\chi^2$	df	P-value
		AS	QS	W			
Bursting	SAT [n/minute]	6.41 (1.80)	6.06 (1.64)	5.98 (1.94)	40.539	2	<0.001 ***
	ISI [seconds]	3.83 (4.37)	5.08 (4.76)	2.60 (2.26)	54.480	2	<0.001 ***
	ISP [%]	47.24 (21.76)	57.14 (18.58)	34.91 (18.50)	212.330	2	<0.001 ***
Synchrony	ASI	6.82 (4.83)	4.76 (3.09)	4.11 (1.70)	1.147	2	0.564
Spectral power	SP_ABS_ $\delta$	1087.41 (810.60)	932.47 (597.82)	888.17 (698.74)	264.720	2	<0.001 ***
	SP_ABS_0	71.46 (62.99)	63.70 (50.58)	75.03 (46.78)	6.330	2	0.042 *
	SP_ABS_ $\alpha$	14.52 (11.02)	12.35 (8.41)	29.92 (32.86)	227.930	2	<0.001 ***
	SP_ABS_ $\beta$	6.20 (8.18)	4.22 (7.59)	29.84 (39.86)	528.800	2	<0.001 ***
	SP_REL_ $\delta$ [%]	0.91 (0.06)	0.92 (0.05)	0.85 (0.10)	75.286	2	<0.001 ***
	SP_REL_0 [%]	0.08 (0.06)	0.07 (0.05)	0.09 (0.04)	9.861	2	0.007 **
	SP_REL_ $\alpha$ [%]	0.02 (0.01)	0.01 (0.01)	0.04 (0.04)	338.640	2	<0.001 ***
	SP_REL_ $\beta$ [%]	0.01 (0.01)	0.00 (0.01)	0.04 (0.05)	483.560	2	<0.001 ***
	Complexity	MSE_AUC	8.62 (2.71)	6.84 (2.38)	12.39 (4.75)	281.750	2
MSE_MAX		0.64 (0.19)	0.52 (0.17)	0.83 (0.25)	238.970	2	<0.001 ***
MSE_SLOPE_F		0.06 (0.02)	0.05 (0.02)	0.09 (0.04)	391.250	2	<0.001 ***
MSE_SLOPE_C		0.02 (0.01)	0.02 (0.01)	0.02 (0.01)	132.960	2	<0.001 ***

\*  $P < 0.05$ , \*\*  $P < 0.01$ , \*\*\*  $P < 0.001$ .

Means were reported with their standard deviation in parentheses. For each qEEG feature a generalized linear mixed model with Wald Chi-square ( $\chi^2$ ) test was used to detect statistically significant differences among different sleep-wake states. The P-value tests the null hypothesis that all the three sleep-wake states have identical mean values for each qEEG feature. The significance threshold was set at  $P < 0.05$ . EEG = electroencephalography; qEEG = quantitative EEG; df = degrees of freedom; AS = active sleep; QS = quiet sleep; W = wake; SAT = spontaneous activity transients; ISI = inter-SAT interval; ISP = percentage of inter-SAT duration per minute; ASI = activation synchrony index; SP\_ABS = absolute spectral power; SP\_REL = relative spectral power;  $\delta$  = delta frequency band; 0 = theta frequency band;  $\alpha$  = alpha frequency band;  $\beta$  = beta frequency band; MSE = multiscale entropy; MSE\_AUC = area under the MSE curve; MSE\_MAX = maximum value of the MSE curve; MSE\_SLOPE\_F = average slope of the MSE curve in fine scales (scale 1–5); MSE\_SLOPE\_C = average slope of the MSE curve in coarse scales (scale 6–20).

pairwise comparison analyses were presented in Supplementary Table S2.

Significant differences between AS and QS were found for all the three bursting features (cf. Fig. 1). Rate of SAT was higher in AS than in QS ( $P < 0.001$ ), while ISI and ISP were lower in AS than in QS (both  $P < 0.001$ ). Rate of SAT was significantly higher in AS than in W ( $P = 0.011$ ) (cf. Fig. 1A). ISI and ISP were significantly higher in QS than in W ( $P = 0.020$ ,  $P < 0.001$ , respectively) (cf. Fig. 1B and 1C).

Out of the four frequency bands, the low-frequency delta band exhibited the highest absolute and relative power values during all sleep states, with theta being the second, and alpha and beta the lowest (Table 2). Higher delta power was observed in either of the sleep states compared to wakefulness, while higher power in other frequency bands was found in wakefulness compared to sleep states. Relative beta power and absolute power of the delta, alpha and beta bands were significantly different between each pair of the three behavioral states (all  $P < 0.001$ ) (cf. Fig. 2A, 2C and 2D). Relative delta and alpha power differed significantly in the state pairs of AS-W and QS-W (all  $P < 0.001$ ) (cf. Fig. 2E and 2G). Significant differences were also found in absolute theta power of AS-QS ( $P = 0.036$ ) (cf. Fig. 2B) and in relative theta power of AS-W ( $P = 0.020$ ) (cf. Fig. 2F).

All MSE features were significantly different between each state pair (all  $P < 0.001$ ), with the area under the MSE curve, the maximum value of the curve, and the average slope of the curve in fine scales following a trend of  $W > AS > QS$ , while the average slope of the curve in coarse scales following a pattern of  $AS > QS > W$  (cf. Fig. 3).

#### 3.3. Effects of age on sleep-qEEG measures

We also tested the influence of age on qEEG measures across different sleep-wake states (Table 3, Supplementary Table S3 and S4). The enrolled infants were divided into two subgroups, EP (<28 wks GA) and VP (28–30 wks GA). Significant age differences were found in SAT, ISP, ASI, relative alpha power, and absolute power of delta, theta and alpha bands. Most remarkably, ASI was significantly higher in AS than in QS for the VP group ( $P < 0.033$ ).

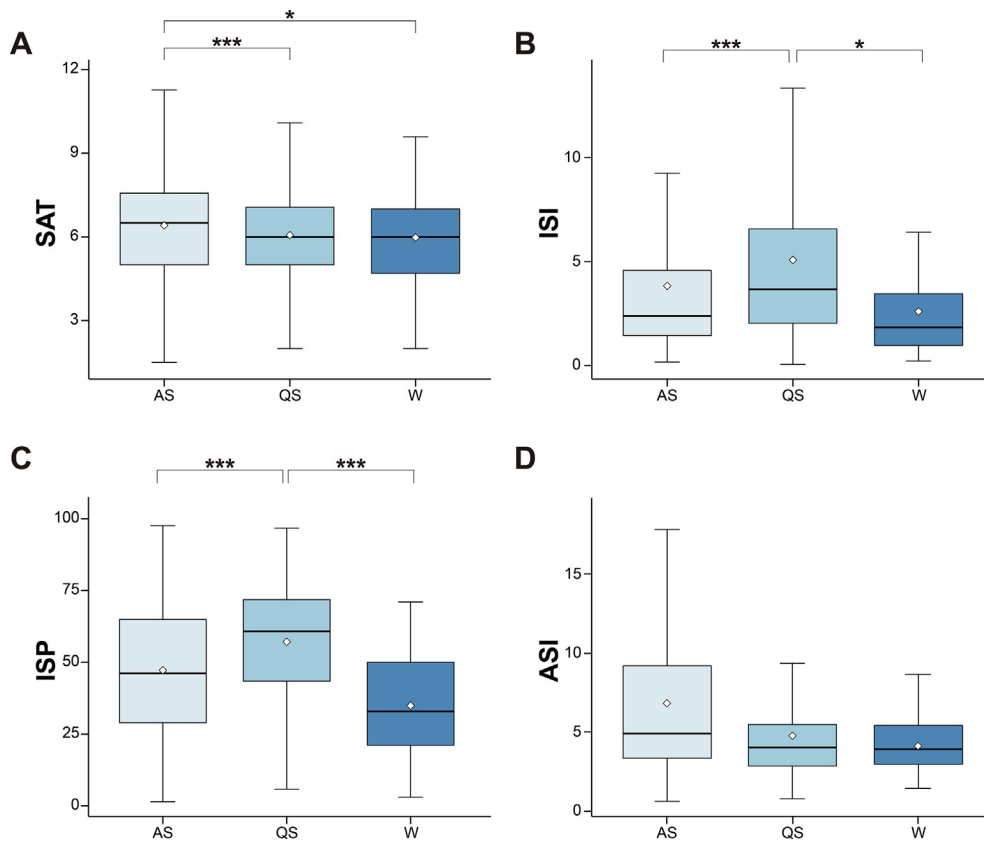


**Fig. 1.** Comparison of EEG bursting and synchrony characteristics (**A**) SAT, (**B**) ISI, (**C**) ISP and (**D**) ASI during different sleep-wake states: AS, QS and W. On each box plot the central horizontal line indicates the median, the upper and lower box bounds represent the third and first quartile respectively, the upper and lower whiskers represent 1.5 times the interquartile range from upper and lower quartile respectively, and the white diamonds denote the mean. Asterisks indicate statistically significant differences among sleep-wake state pairs (\*  $P < 0.05$ , \*\*  $P < 0.01$ , \*\*\*  $P < 0.001$ , Holm corrected for multiple comparisons). EEG = electroencephalography; SAT = spontaneous activity transients; ISI = inter-SAT interval; ISP = percentage of inter-SAT duration per minute; ASI = activation synchrony index; AS = active sleep; QS = quiet sleep; W = wake.

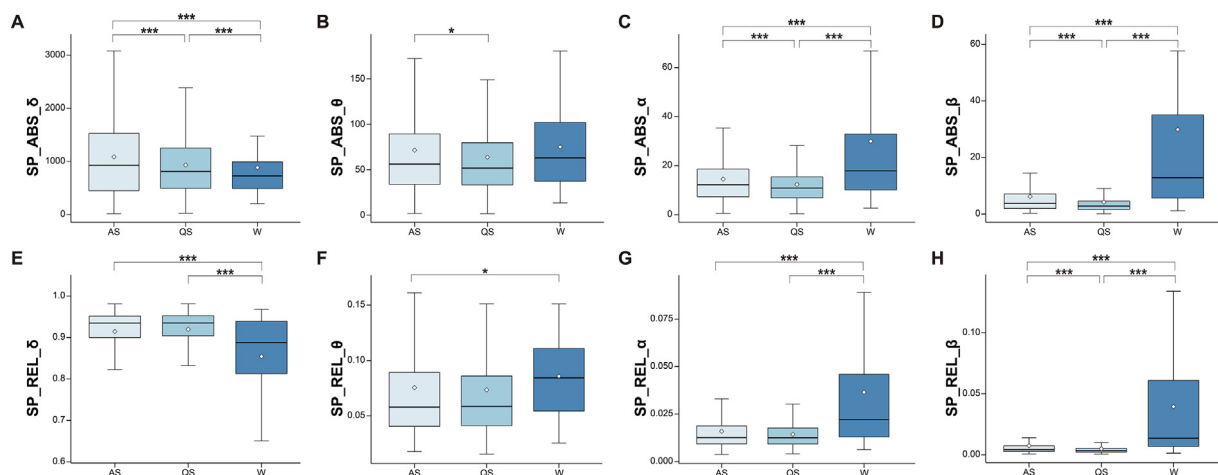


**Fig. 2.** Comparison of EEG spectral power characteristics (**A**) SP\_ABS\_δ, (**B**) SP\_ABS\_θ, (**C**) SP\_ABS\_α, (**D**) SP\_ABS\_β, (**E**) SP\_REL\_δ, (**F**) SP\_REL\_θ, (**G**) SP\_REL\_α and (**H**) SP\_REL\_β during different sleep-wake states: AS, QS and W. On each box plot the central horizontal line indicates the median, the upper and lower box bounds represent the third and first quartile respectively, the upper and lower whiskers represent 1.5 times the interquartile range from upper and lower quartile respectively, and the white diamonds denote the mean. Asterisks indicate statistically significant differences among sleep-wake state pairs (\*  $P < 0.05$ , \*\*  $P < 0.01$ , \*\*\*  $P < 0.001$ , Holm corrected for multiple comparisons). EEG = electroencephalography; SP\_ABS = absolute spectral power; SP\_REL = relative spectral power; δ = delta frequency band; θ = theta frequency band; α = alpha frequency band; β = beta frequency band; AS = active sleep; QS = quiet sleep; W = wake.

### 3.4. Automated sleep stage classification using qEEG features

The MLR classifier based on the combination of all qEEG features reached a mean AUC of 0.748 (SD = 0.065,  $P < 0.001$ ) and a

mean accuracy of 0.658 (SD = 0.041,  $P < 0.001$ ) (cf. Fig. 4). The most contributing features for recognizing AS, QS and W were the maximum value of the MSE curve, the area under the MSE curve, and the average slope of the MSE curve in fine scales, respectively.

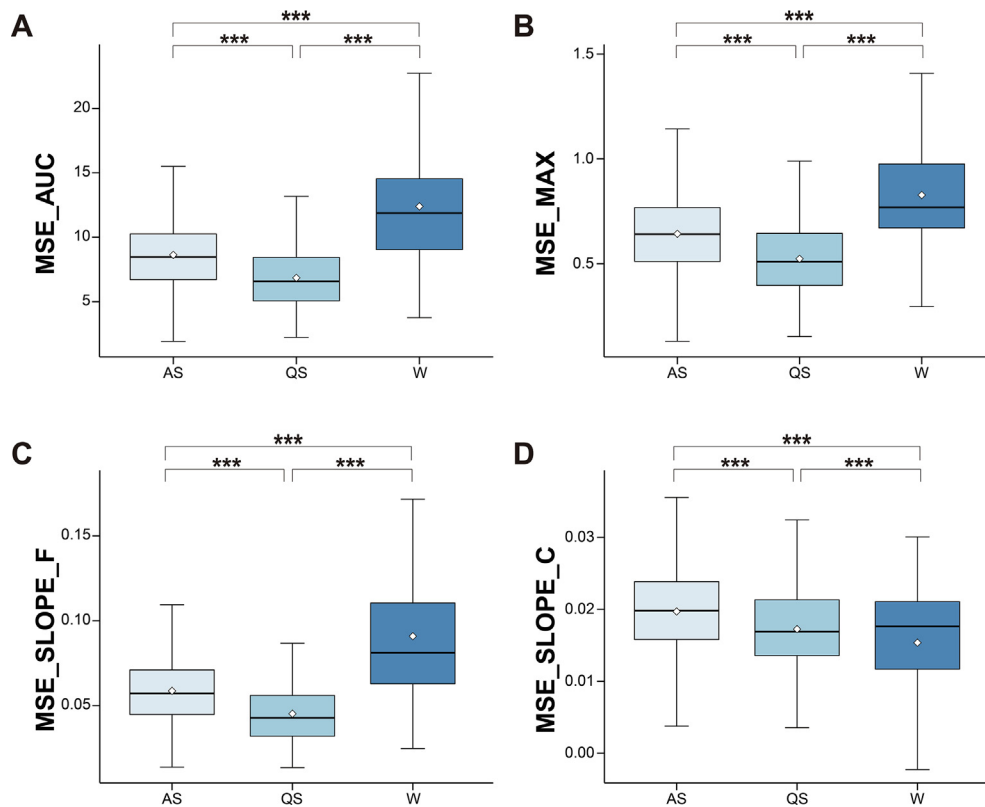


**Fig. 3.** Comparison of EEG complexity characteristics (A) MSE\_AUC, (B) MSE\_MAX, (C) MSE\_SLOPE\_F and (D) MSE\_SLOPE\_C during different sleep-wake states: AS, QS and W. On each box plot the central horizontal line indicates the median, the upper and lower box bounds represent the third and first quartile respectively, the upper and lower whiskers represent 1.5 times the interquartile range from upper and lower quartile respectively, and the white diamonds denote the mean. Asterisks indicate statistically significant differences among sleep-wake state pairs (\*  $P < 0.05$ , \*\*  $P < 0.01$ , \*\*\*  $P < 0.001$ , Holm corrected for multiple comparisons). EEG = electroencephalography; MSE = multiscale entropy; MSE\_AUC = area under the MSE curve; MSE\_MAX = maximum value of the MSE curve; MSE\_SLOPE\_F = average slope of the MSE curve in fine scales (scale 1–5); MSE\_SLOPE\_C = average slope of the MSE curve in coarse scales (scale 6–20); AS = active sleep; QS = quiet sleep; W = wake.

**Table 3**  
GLMM results for age  $\times$  sleep-wake states interaction effects on qEEG measures.

Feature type	Feature	Wald $\chi^2$	df	P-value
Bursting	SAT [n/minute]	19.247	2	<0.001 ***
	ISI [seconds]	2.388	2	0.303
	ISP [%]	7.969	2	0.019 *
Synchrony	ASI	8.031	2	0.018 *
Spectral power	SP_ABS_ $\delta$	20.661	2	<0.001 ***
	SP_ABS_ $\theta$	3,582,376	2	<0.001 ***
	SP_ABS_ $\alpha$	15.263	2	<0.001 ***
	SP_ABS_ $\beta$	3.928	2	0.140
	SP_REL_ $\delta$ [%]	2.585	2	0.275
	SP_REL_ $\theta$ [%]	1.859	2	0.395
	SP_REL_ $\alpha$ [%]	18.482	2	<0.001 ***
	SP_REL_ $\beta$ [%]	1.157	2	0.561
	Complexity	MSE_AUC	2.269	2
MSE_MAX		1.025	2	0.599
MSE_SLOPE_F		6.990	2	0.030 *
MSE_SLOPE_C		0.408	2	0.816

\*  $P < 0.05$ , \*\*  $P < 0.01$ , \*\*\*  $P < 0.001$ .

Means were reported with their standard deviation in parentheses. For each qEEG feature a generalized linear mixed model with Wald Chi-square ( $\chi^2$ ) test was used to determine whether the interaction effect of age  $\times$  sleep-wake states is statistically significant. The significance threshold was set at  $P < 0.05$ . GLMM = generalized linear mixed model; EEG = electroencephalography; qEEG = quantitative EEG; df = degrees of freedom; AS = active sleep; QS = quiet sleep; W = wake; SAT = spontaneous activity transients; ISI = inter-SAT interval; ISP = percentage of inter-SAT duration per minute; ASI = activation synchrony index; SP\_ABS = absolute spectral power; SP\_REL = relative spectral power;  $\delta$  = delta frequency band;  $\theta$  = theta frequency band;  $\alpha$  = alpha frequency band;  $\beta$  = beta frequency band; MSE = multiscale entropy; MSE\_AUC = area under the MSE curve; MSE\_MAX = maximum value of the MSE curve; MSE\_SLOPE\_F = average slope of the MSE curve in fine scales (scale 1–5); MSE\_SLOPE\_C = average slope of the MSE curve in coarse scales (scale 6–20).

We further compared the individual predictive power of each kind of feature by building four independent MLR models. The complexity (i.e., MSE) feature subset yielded the best AUC, which is close to

the predictive ability of all kinds of feature collection (cf. Fig. 5). The classification performance was also significant for EP (accuracy =  $0.664 \pm 0.045$ ,  $P < 0.001$ ; AUC =  $0.762 \pm 0.077$ ,

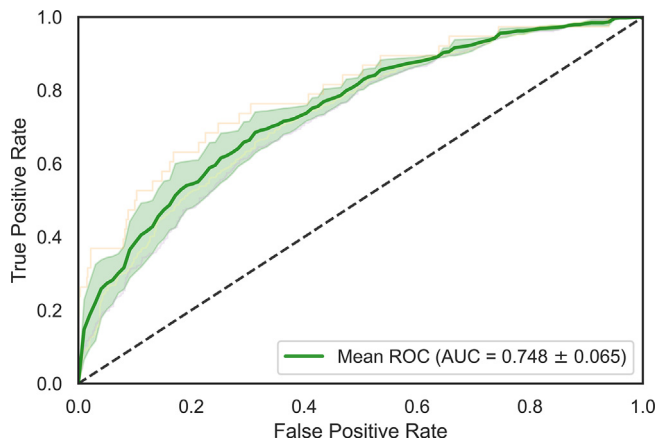


**Fig. 4.** The ROC curve of the multinomial logistic regression combined with a repeated 10-fold cross-validation procedure. Macro-averaged AUC value is reported with its standard deviation in parentheses. ROC = receiver operating characteristic; AUC = area under the curve.

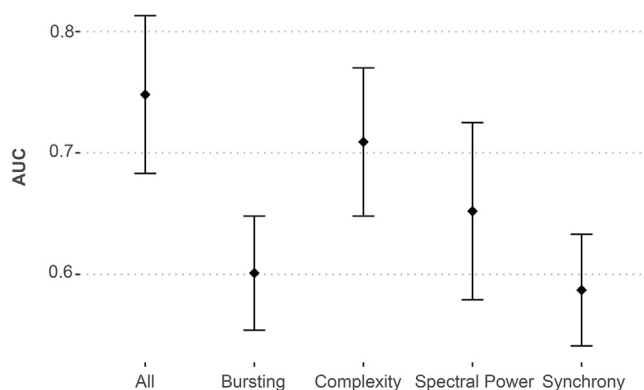


**Fig. 5.** Comparison of AUCs obtained from MLR models using the collection of all qEEG features and different kinds of feature subsets. On each error bar the central black diamonds indicate the mean, and the upper and lower whiskers represent 1 standard deviation above and below the mean, respectively. AUC = area under the curve; MLR = multinomial logistic regression; qEEG = quantitative electroencephalography.

$P < 0.001$ ) and VP (accuracy =  $0.665 \pm 0.065$ ,  $P < 0.001$ ; AUC =  $0.713 \pm 0.105$ ,  $P < 0.001$ ) subgroups, separately.

#### 4. Discussion

Using quantitative analysis of dual-channel EEG, the current study characterized the distributions of a set of representative qEEG measures across different behavioral sleep-wake states (AS, QS, and W) for extremely and very preterm infants (<30 wks GA) during their first three days after birth. Our results showed that most (15/16, 94 %) qEEG features differed significantly between sleep-wake states in the entire sample. The exception was the synchrony feature (i.e., ASI) which only differed significantly between AS and QS in the very preterm subgroup (28–30 wks GA). In addition to ASI, sleep-bursting and sleep-spectral power associations were also found to be influenced by age. Furthermore, the combination of all qEEG features achieved good automated sleep-wake state classification performance.

The results of bursting analyses showed that SAT rate was significantly higher in AS than in QS, while ISP and ISI were higher in QS than in AS. Similar results were also reported by Palmu et al. (2013), who found that the proportion of SAT events was dif-

ferent between PSG-defined sleep stages, with AS > QS. Moreover, our findings agree well with existing visual EEG assessment findings that QS and AS are characterized by discontinuous and relatively continuous background EEG activity, respectively (André et al., 2010; Bourel-Ponchel et al., 2020; Dereymaeker, Pillay, Vervisch, De Vos, et al., 2017). A growing body of evidence has now demonstrated the critical importance of SAT events in early human brain development (Arichi et al., 2017; Benders et al., 2015; O'Toole et al., 2016; Tolonen et al., 2007; Vanhatalo and Kaila, 2006). The result of higher SAT in AS than in QS thus lend further support to the present notion that AS, as compared to QS, might contribute more to the early developmental processes (Graven and Browne, 2008; Mirmiran, 1995; Mirmiran et al., 2003). To promote optimal brain development, it is of particular importance for caregivers to safeguard AS in the NICU settings.

Despite the significant sleep-bursting associations, it appeared that the state of wakefulness could not be well characterized by the bursting features in the current sample. Both lowest SAT rate and inter-SAT (ISI and ISP) values were seen during wakefulness (cf. Fig. 1). This is paradoxical, as SAT and inter-SAT measures are negatively correlated. One possible explanation for this paradoxical finding is that the small number of waking states observed in the current study could not adequately represent the actual situation.

Regarding the degree of interhemispheric synchrony, we found lower ASI values during all three sleep-wake states in VP infants compared to EP infants (Supplementary Table S3). This result is in line with previous visual EEG studies in which high synchrony between the two hemispheres was consistently observed before 28 wks GA, followed by asynchronous bursting activity until near-term age (André et al., 2010; Hrachovy and Mizrahi, 2015). The early synchronizations occurring in EP infants are believed to reflect non-synaptic communication (Bourel-Ponchel et al., 2020; Wallois et al., 2021). So far, no evidence exists that transitions between sleep states drive changes in non-synaptic activities in EP infants, which might be the cause for non-significant sleep-ASI associations in this subgroup. The subsequent asynchrony in older preterm infants is considered to be caused by the fact that the generation of non-synaptic events is massively attenuated, and the developing callosal fibers are not yet mature enough to produce stable interhemispheric interactions (Wallois et al., 2021). The synaptic plasticity has long been postulated to be facilitated by AS during early brain development (Del Rio-Bermudez and Blumberg, 2018; Knoop et al., 2021; Kurth et al., 2015; Li et al., 2017; Liu et al., 2007). Hence, it is reasonably speculated that the significantly higher ASI value in AS compared to QS, as found in the subgroup of VP infants, is related to callosal synaptic development.

Additionally, Räsänen et al. (2013) found that ASI could not well represent continuous activity during AS in an older preterm cohort with average conceptional age of 30.4 weeks. This, however, appears to have little discernible impact on the present study, since the EEG itself is almost completely constituted by a discontinuous background in all behavioral states (relatively more continuous in AS than in QS) in preterm infants born before 30 wks GA (André et al., 2010). Future studies should consider the fact that the use of ASI might lead to controversial results in older infants with more continuous EEG background activity, especially during AS.

In accordance with existing preterm EEG evidence, the power spectral analyses revealed an imbalance between low- and high-frequency content. For all sleep-wake states, the overwhelming majority (above 85 %) of overall spectral power was concentrated in the low-frequency delta band. Slow delta waves with superimposed fast activity (i.e., 8- to 30-Hz alpha-beta spindles), also known as “delta brushes”, are the hallmark of preterm EEG and constitute the main component of the SATs (Milh et al., 2007;

Pavlidis et al., 2017; Vecchierini et al., 2007). During the early preterm period, delta brushes occur more in AS than in QS (Vanhatalo and Kaila, 2006; Whitehead et al., 2016), which explains the significantly higher power of the delta, alpha and beta bands during AS compared to QS, as observed in the present work.

Higher-frequency components, primarily alpha and beta bands, of neonatal EEG signals have been associated with the processing of exogenous or environmental stimuli during wakefulness (Norman et al., 2008; Saby and Marshall, 2012). Given that infants' brain shows less EEG activity while asleep than awake, it is not surprising to see higher alpha and beta power in wake than in either of the sleep states. Interestingly, there is evidence that neonates are capable of learning and processing external information even during sleep, particularly AS (Fifer et al., 2010; Tarullo et al., 2011). This could also be the reason for the higher alpha and beta power observed in AS than in QS.

The theta power was of limited value for differentiating between sleep-wake states in the entire group (cf. Fig. 2B and 2F). However, most pairwise comparison analyses of theta power reached statistical significance for the EP and VP subgroups, separately (Supplementary Table S4). Previous research suggested that the evolution of theta activities depends upon subsequent activation of endogenous generators (Wallosis et al., 2021). The drivers of these generators change at around 28 wks GA (i.e., the boundary between EP and VP subgroups) from spontaneous activities to sensory information. Therefore, it would be attractive to speculate that different generator-based mechanisms underlie the association between theta power and sleep-wake states in extremely and very preterm infants.

The complexity index (i.e., the area under the MSE curve) was highest in W but decreased in AS and reached its lowest level during QS, reflecting the high-to-low level of brain activity associated with each sleep/wake state (Ma et al., 2018). The fine-scale slope of the MSE curve and the maximum value of the curve showed a similar distribution pattern across the three states. In contrast, at coarse time scale, the slope of the MSE curve followed a distinct pattern of AS > QS > W. These results indicate a time scale-specific relationship between entropy and sleep-wake states, which was also seen in healthy adults (Miskovic et al., 2019; Shi et al., 2017). Furthermore, fine-to-coarse time scales of MSE were assumed to be linked to power content in terms of high-to-low frequencies, respectively (Courtiol et al., 2016). This explains the same distribution pattern found for finer-scale MSE and higher frequency power (W > AS > QS), and the same pattern for coarser-scale MSE and lower frequency power (AS > QS > W).

Despite the noticeable impact of maturational effects on some of the above-mentioned qEEG features, we found that automated sleep staging is possible in extremely and very preterm infants by combining these different features together. The classification performance (overall AUC = 0.748) is comparable to, or even better than existing automated sleep staging algorithms based on multi-channel qEEG in the same population, which were implemented during a later postnatal period (i.e., a few weeks after birth) (De Wel et al., 2017; Dereymaeker, Pillay, Vervisch, Van Huffel, et al., 2017; Koolen et al., 2017). In addition, we found that MSE metrics are the most important features in automated sleep staging, irrespective of age, which implies their greater robustness and reliability compared to other qEEG measures used in the present study. Although the MSE analysis is still rarely applied to preterm EEG, our findings show it as a promising avenue for future studies on better characterizing sleep-wake states and as a useful index applied across different preterm age groups.

Several limitations of this study warrant mention. To achieve reliable estimates of sleep-qEEG patterns, we conducted successive behavioral observations over a period of three hours, covering several complete sleep cycles (André et al., 2010), in relatively healthy

infants who were clinically stable at the time of observation. However, this resulted in a small sample size ( $n = 17$ ), which may reduce the statistical power to draw firm inferences. Furthermore, as sleep pervades preterm newborn's life, only a small number of waking states were observed in the current sample. More awake data is needed for further confirmation of our findings on wakefulness in future work. Another point of concern is the restricted visibility of behaviors in several infants, due to respiratory support or phototherapy during sleep observation (Supplementary Table S1). These conditions led to fewer parameters available to score sleep stages confidently. This issue can be mitigated by the sleep annotation smoothing procedure used in the current study but cannot be entirely excluded. Moreover, a clear sleep state distinction is known to be quite difficult in preterm infants born at less than 30 wks GA, which might inherently limit the sleep classification performance (Barbeau and Weiss, 2017; Bennet et al., 2018; Kuhle et al., 2001).

It is worth highlighting several promising directions for future research. Firstly, despite the use of cross-validation in the current study, an independent external validation sample would help enhance the generalizability (i.e., external validity) of our findings. In the future, we will explore a web-accessible implementation of our analysis procedure, creating an opportunity for NICU clinicians and researchers to validate our qEEG-based automated sleep staging model in their own practice. Secondly, aiming to provide guideline values for clinicians, the present study only included a limited number of typical qEEG features. To create a fully automated sleep classification system in the NICU, future research should consider using a more extensive and comprehensive qEEG feature set. In particular, a basic assumption of the spectral analysis is the stationarity of data, which is not well fulfilled due to the non-stationary nature of neonatal EEG. Future research could apply more advanced time-frequency techniques to improve the time-varying EEG spectral estimation. Finally, state-of-the-art EEG techniques, such as dry electrodes and cable shielding, are being developed for early preterm infants, which would further increase the clinical utility of the present work in the future.

## 5. Conclusion

In sum, we demonstrated the feasibility of differentiating sleep-wake states using quantitative analysis of dual-channel EEG in preterm infants born before 30 wks GA during their first three days after birth. The fusion of different qEEG features enabled automated sleep-wake state classification with achieving a good prediction performance in both EP and VP infants. Complexity characteristics showed the strongest predictive power among the four kinds of qEEG parameters and might be the most promising and valuable features for future preterm sleep-EEG research. Our findings may provide a promising solution for creating a completely automated sleep assessment tool that assists appropriate care planning in the NICU, thereby enhancing neurodevelopmental outcomes for extremely and very preterm infants.

## Declaration of Competing Interest

The authors declare that they have no conflict of interest.

## Acknowledgements

This work was supported by the European Commission [Grant agreement number: EU H2020 MSCA-ITN-2018-#813483, INtegrating Functional Assessment measures for Neonatal Safeguard (INFANS)].



## Appendix A. Supplementary material

Supplementary data to this article can be found online at <https://doi.org/10.1016/j.clinph.2022.11.018>.

## References

- Als H, McAnulty GB. The Newborn Individualized Developmental Care and Assessment Program (NIDCAP) with Kangaroo Mother Care (KMC): Comprehensive Care for Preterm Infants. *Curr Womens Health Rev* 2011;7(3):288–301. <https://doi.org/10.2174/157340411796355216>.
- Altamir L, Phillips R. The Neonatal Integrative Developmental Care Model: Advanced Clinical Applications of the Seven Core Measures for Neuroprotective Family-centered Developmental Care. *Newborn Infant Nurs Rev* 2016;16(4):230–44. <https://doi.org/10.1053/j.nainr.2016.09.030>.
- Anders TF, Keener MA, Kraemer H. Sleep-wake state organization, neonatal assessment and development in premature infants during the first year of life. *II. Sleep* 1985;8(3):193–206.
- André M, Lamblin M-D, d'Allest AM, Curzi-Dascalova L, Moussalli-Salefranque F, Nguyen The Tich S, et al. Electroencephalography in premature and full-term infants. Developmental features and glossary. *Neurophysiol. Clin Neurophysiol* 2010;40(2):59–124. <https://doi.org/10.1016/j.neucli.2010.02.002>.
- Arichi T, Whitehead K, Barone G, Pressler R, Padormo F, Edwards AD, et al. Localization of spontaneous bursting neuronal activity in the preterm human brain with simultaneous EEG-fMRI. *Elife* 2017;6:e27814.
- Barbeau DY, Weiss MD. Sleep Disturbances in Newborns. *Children (Basel)* 2017;4(10):90. <https://doi.org/10.3390/children4100090>.
- Benders MJ, Palmu K, Menache C, Borradori-Tolsa C, Lazeyras F, Sizonenko S, et al. Early Brain Activity Relates to Subsequent Brain Growth in Premature Infants. *Cereb Cortex* 2015;25(9):3014–24. <https://doi.org/10.1093/cercor/bhu097>.
- Bennet L, Walker DW, Horne RSC. Waking up too early – the consequences of preterm birth on sleep development. *J Physiol* 2018;596(23):5687–708. <https://doi.org/10.1113/JP274950>.
- Bik A, Sam C, de Groot ER, Visser SSM, Wang X, Tataranno ML, et al. A scoping review of behavioral sleep stage classification methods for preterm infants. *Sleep Med* 2022;90:74–82. <https://doi.org/10.1016/j.sleep.2022.01.006>.
- Bourel-Ponchel E, Gueden S, Hasaerts D, Héberlé C, Malfilâtre G, Mony L, et al. Normal EEG during the neonatal period: maturational aspects from premature to full-term newborns. *Neurophysiol Clin* 2020;51(1):61–88.
- Brazelton TB, Nugent JK. Neonatal behavioral assessment scale (Issue 137). Cambridge University Press; 1995.
- Costa M, Goldberger AL, Peng C-K. Multiscale Entropy Analysis of Complex Physiologic Time Series. *Phys Rev Lett* 2002;89(6):68102. <https://doi.org/10.1103/PhysRevLett.89.068102>.
- Costa M, Goldberger AL, Peng C-K. Multiscale entropy analysis of biological signals. *Phys Rev E* 2005;71(2):21906. <https://doi.org/10.1103/PhysRevE.71.021906>.
- Courtiol J, Perdakis D, Petkoski S, Müller V, Huys R, Sleimen-Malkoun R, et al. The multiscale entropy: Guidelines for use and interpretation in brain signal analysis. *J Neurosci Methods* 2016;273:175–90. <https://doi.org/10.1016/j.jneumeth.2016.09.004>.
- de Groot ER, Bik A, Sam C, Wang X, Shellhaas RA, Austin T, et al. Creating an optimal observational sleep stage classification system for very and extremely preterm infants. *Sleep Med* 2022;90:167–75. <https://doi.org/10.1016/j.sleep.2022.01.020>.
- De Wel O, Lavanga M, Dorado AC, Jansen K, Dereyemaeker A, Naulaers G, et al. Complexity Analysis of Neonatal EEG Using Multiscale Entropy: Applications in Brain Maturation and Sleep Stage Classification. *Entropy* 2017;19(10):516. <https://doi.org/10.3390/e19100516>.
- De Wel O, Van Huffel S, Lavanga M, Jansen K, Dereyemaeker A, Dudink J, et al. Relationship Between Early Functional and Structural Brain Developments and Brain Injury in Preterm Infants. *Cerebellum* 2021;20(4):556–68. <https://doi.org/10.1007/s12311-021-01232-z>.
- Del Rio-Bermudez C, Blumberg MS. Active Sleep Promotes Functional Connectivity in Developing Sensorimotor Networks. *Bioessays* 2018;40(4):e1700234–e. <https://doi.org/10.1002/bies.201700234>.
- Dereyemaeker A, Pillay K, Vervisch J, De Vos M, Van Huffel S, Jansen K, et al. Review of sleep-EEG in preterm and term neonates. *Early Hum Dev* 2017a;113:87–103. <https://doi.org/10.1016/j.earlhumdev.2017.07.003>.
- Dereyemaeker A, Pillay K, Vervisch J, Van Huffel S, Naulaers G, Jansen K, et al. An Automated Quiet Sleep Detection Approach in Preterm Infants as a Gateway to Assess Brain Maturation. *Int J Neural Syst* 2017b;27(6):1750023. <https://doi.org/10.1142/S012906571750023X>.
- Fifer WP, Byrd DL, Kaku M, Eigsti I-M, Isler JR, Grose-Fifer J, et al. Newborn infants learn during sleep. *Proc Natl Acad Sci U S A* 2010;107(22):10320–3. <https://doi.org/10.1073/pnas.1005061107>.
- Georgoulas A, Jones L, Laudiano-Dray MP, Meek J, Fabrizi L, Whitehead K. Sleep-wake regulation in preterm and term infants. *Sleep* 2021;44(1):zsa148. <https://doi.org/10.1093/sleep/zsaa148>.
- Graven SN, Browne JV. Sleep and Brain Development: The Critical Role of Sleep in Fetal and Early Neonatal Brain Development. *Newborn Infant Nurs Rev* 2008;8(4):173–9. <https://doi.org/10.1053/j.nainr.2008.10.008>.
- Grigg-Damberger M, Gozal D, Marcus CL, Quan SF, Rosen CL, Chervin RD, et al. The visual scoring of sleep and arousal in infants and children. *J Clin Sleep Med* 2007;3(02):201–40.
- Hrachovy RA, Mizrahi EM. Atlas of neonatal electroencephalography. Springer Publishing Company; 2015.
- Humberg A, Fortmann I, Siller B, Kopp MV, Herting E, Göpel W, et al. Preterm birth and sustained inflammation: consequences for the neonate. *Semin Immunopathol* 2020;42(4):451–68. <https://doi.org/10.1007/s00281-020-00803-z>.
- Jasper HH. The ten-twenty electrode system of the International Federation. *Electroencephalogr Clin Neurophysiol* 1958;10:370–5.
- Knoop MS, de Groot ER, Dudink J. Current ideas about the roles of rapid eye movement and non-rapid eye movement sleep in brain development. *Acta Paediatr* 2021;110(1):36–44.
- Koolen N, Dereyemaeker A, Räsänen O, Jansen K, Vervisch J, Matic V, et al. Interhemispheric synchrony in the neonatal EEG revisited: activation synchrony index as a promising classifier. *Front Hum Neurosci* 2014;8:1030. <https://www.frontiersin.org/article/10.3389/fnhum.2014.01030>.
- Koolen N, Oberdorfer L, Rona Z, Giordano V, Werther T, Klebermass-Schrehof K, et al. Automated classification of neonatal sleep states using EEG. *Clin Neurophysiol* 2017;128(6):1100–8. <https://doi.org/10.1016/j.clinph.2017.02.025>.
- Kosciessa JQ, Kloosterman NA, Garrett DD. Standard multiscale entropy reflects neural dynamics at mismatched temporal scales: What's signal irregularity got to do with it? *PLoS Comput Biol* 2020;16(5):e1007885–e. <https://doi.org/10.1371/journal.pcbi.1007885>.
- Kuhle S, Klebermass K, Ollischar M, Hulek M, Prusa AR, Kohlhauser C, et al. Sleep-wake cycles in preterm infants below 30 weeks of gestational age. Preliminary results of a prospective amplitude-integrated EEG study. *Wien Klin Wochenschr* 2001;113(7–8):219–23.
- Kurth S, Olini N, Huber R, LeBourgeois M. Sleep and Early Cortical Development. *Curr Sleep Med Reports* 2015;1(1):64–73. <https://doi.org/10.1007/s40675-014-0002-8>.
- Li W, Ma L, Yang G, Gan W-B. REM sleep selectively prunes and maintains new synapses in development and learning. *Nat Neurosci* 2017;20(3):427–37. <https://doi.org/10.1038/nn.4479>.
- Liu WF, Laudert S, Perkins B, MacMillan-York E, Martin S, et al. The development of potentially better practices to support the neurodevelopment of infants in the NICU. *J Perinatol* 2007;27(S2):S48–74.
- Louis EKS, Frey LC, Britton JW, Hopp JL, Korb P, Koubeissi MZ, et al. The Normal EEG. *Electroencephalography (EEG): An Introductory Text and Atlas of Normal and Abnormal Findings in Adults, Children, and Infants [Internet]*. American Epilepsy Society; 2016.
- Ma Y, Shi W, Peng C-K, Yang AC. Nonlinear dynamical analysis of sleep electroencephalography using fractal and entropy approaches. *Sleep Med Rev* 2018;37:85–93. <https://doi.org/10.1016/j.smrv.2017.01.003>.
- Milh M, Kaminska A, Huon C, Lapillonne A, Ben-Ari Y, Khazipov R. Rapid Cortical Oscillations and Early Motor Activity in Premature Human Neonate. *Cereb Cortex* 2007;17(7):1582–94. <https://doi.org/10.1093/cercor/bhl069>.
- Mirmiran M. The function of fetal/neonatal rapid eye movement sleep. *Behav Brain Res* 1995;69(1):13–22. [https://doi.org/10.1016/0166-4328\(95\)00019-P](https://doi.org/10.1016/0166-4328(95)00019-P).
- Mirmiran M, Maas YGH, Ariagno RL. Development of fetal and neonatal sleep and circadian rhythms. *Sleep Med Rev* 2003;7(4):321–34. <https://doi.org/10.1053/smr.2002.0243>.
- Miskovic V, MacDonald KJ, Rhodes LJ, Cote KA. Changes in EEG multiscale entropy and power-law frequency scaling during the human sleep cycle. *Hum Brain Mapp* 2019;40(2):538–51. <https://doi.org/10.1002/hbm.24393>.
- Norman E, Rosén I, Vanhatalo S, Stjernqvist K, Ökland O, Fellman V, et al. Electroencephalographic Response to Procedural Pain in Healthy Term Newborn Infants. *Pediatr Res* 2008;64(4):429–34. <https://doi.org/10.1203/PDR.0b013e3181825487>.
- O'Toole JM, Boylan GB. Quantitative Preterm EEG Analysis: The Need for Caution in Using Modern Data Science Techniques. *Front Pediatr* 2019;7:174. <https://doi.org/10.3389/fped.2019.00174>.
- O'Toole JM, Boylan GB, Vanhatalo S, Stevenson NJ. Estimating functional brain maturity in very and extremely preterm neonates using automated analysis of the electroencephalogram. *Clin Neurophysiol* 2016;127(8):2910–8. <https://doi.org/10.1016/j.clinph.2016.02.024>.
- O'Toole JM, Pavlidis E, Korotchkova I, Boylan GB, Stevenson NJ. Temporal evolution of quantitative EEG within 3 days of birth in early preterm infants. *Sci Rep* 2019;9(1):4859. <https://doi.org/10.1038/s41598-019-41227-9> PMID = 30890761.
- Palmu K, Kirjavainen T, Stjerna S, Salokivi T, Vanhatalo S. Sleep wake cycling in early preterm infants: Comparison of polysomnographic recordings with a novel EEG-based index. *Clin Neurophysiol* 2013;124(9):1807–14. <https://doi.org/10.1016/j.clinph.2013.03.010>.
- Palmu K, Stevenson N, Wikström S, Hellström-Westas L, Vanhatalo S, Palva JM. Optimization of an NLEO-based algorithm for automated detection of spontaneous activity transients in early preterm EEG. *Physiol Meas* 2010;31(11):N85–93. <https://doi.org/10.1088/0967-3334/31/11/n02>.
- Paul K, Krajča V, Roth Z, Melichar J, Petránek S. Comparison of quantitative EEG characteristics of quiet and active sleep in newborns. *Sleep Med* 2003;4(6):543–52. <https://doi.org/10.1016/j.sleep.2003.08.008>.
- Pavlidis E, Lloyd RO, Mathieson S, Boylan GB. A review of important electroencephalogram features for the assessment of brain maturation in premature infants. *Acta Paediatr* 2017;106(9):1394–408. <https://doi.org/10.1111/apa.13956>.
- Petch J, Di S, Nelson W. Opening the black box: the promise and limitations of explainable machine learning in cardiology. *Can J Cardiol* 2021;38(2):204–13.

- Pierrat V, Marchand-Martin L, Marret S, Arnaud C, Benhammou V, Cambonie G, et al. Neurodevelopmental outcomes at age 5 among children born preterm: EPIPAGE-2 cohort study. *BMJ* 2021;373. <https://doi.org/10.1136/bmj.n741>
- Prechtl HFR. The behavioural states of the newborn infant (a review). *Brain Res* 1974;76(2):185–212.
- Räsänen O, Metsäranta M, Vanhatalo S. Development of a novel robust measure for interhemispheric synchrony in the neonatal EEG: Activation Synchrony Index (ASI). *Neuroimage* 2013;69:256–66. <https://doi.org/10.1016/j.neuroimage.2012.12.017>.
- Rice D., Jr S.B. Critical periods of vulnerability for the developing nervous system: evidence from humans and animal models. *Environ Health Perspect*, 2000; 108 (suppl 3), 511–533. <https://doi.org/10.1289/ehp.00108s3511> PMID - 10852851.
- Saby JN, Marshall PJ. The utility of EEG band power analysis in the study of infancy and early childhood. *Dev Neuropsychol* 2012;37(3):253–73. <https://doi.org/10.1080/87565641.2011.614663>.
- Shellhaas RA, Chang T, Tsuchida T, Scher MS, Riviello JJ, Abend NS, et al. The American Clinical Neurophysiology Society's Guideline on Continuous Electroencephalography Monitoring in Neonates. *J Clin Neurophysiol* 2011;28(6):611–7. <https://doi.org/10.1097/wmp.0b013e31823e96d7>.
- Shi W, Shang P, Ma Y, Sun S, Yeh C-H. A comparison study on stages of sleep: Quantifying multiscale complexity using higher moments on coarse-graining. *Commun Nonlinear Sci Numer Simul* 2017;44:292–303. <https://doi.org/10.1016/j.cnsns.2016.08.019>.
- Stevenson NJ, Oberdorfer L, Tataranno M, Breakspear M, Colditz PB, Vries LS, et al. Automated cot-side tracking of functional brain age in preterm infants. *Ann Clin Transl Neurol* 2020;7(6):891–902. <https://doi.org/10.1002/acn3.51043> PMID - 32368863.
- Tao JD, Mathur AM. Using amplitude-integrated EEG in neonatal intensive care. *J Perinatol* 2010;30(1):S73–81. <https://doi.org/10.1038/jp.2010.93>.
- Tarullo AR, Balsam PD, Fifer WP. Sleep and Infant Learning. *Infant Child Dev* 2011;20(1):35–46. <https://doi.org/10.1002/icd.685>.
- Tau GZ, Peterson BS. Normal Development of Brain Circuits. *Neuropsychopharmacology* 2010;35(1):147–68. <https://doi.org/10.1038/npp.2009.115> PMID - 19794405.
- Tokariev A, Palmu K, Lano A, Metsäranta M, Vanhatalo S. Phase synchrony in the early preterm EEG: Development of methods for estimating synchrony in both oscillations and events. *Neuroimage* 2012;60(2):1562–73. <https://doi.org/10.1016/j.neuroimage.2011.12.080>.
- Tolonen M, Palva JM, Andersson S, Vanhatalo S. Development of the spontaneous activity transients and ongoing cortical activity in human preterm babies. *Neuroscience* 2007;145(3):997–1006. <https://doi.org/10.1016/j.neuroscience.2006.12.070>.
- Tong S, Thankor NV. *Quantitative EEG analysis methods and clinical applications*. Artech House; 2009.
- Tsuchida TN, Wusthoff CJ, Shellhaas RA, Abend NS, Hahn CD, Sullivan JE, et al. American clinical neurophysiology society standardized EEG terminology and categorization for the description of continuous EEG monitoring in neonates: report of the American Clinical Neurophysiology Society critical care monitoring committee. *J Clin Neurophysiol* 2013;30(2):161–73.
- Vanhatalo S, Kaila K. Development of neonatal EEG activity: From phenomenology to physiology. *Semin Fetal Neonatal Med* 2006;11(6):471–8. <https://doi.org/10.1016/j.siny.2006.07.008>.
- Vecchierini M-F, André M, d'Allest AM. Normal EEG of premature infants born between 24 and 30 weeks gestational age: Terminology, definitions and maturation aspects. *Neurophysiol Clin Neurophysiol* 2007;37(5):311–23. <https://doi.org/10.1016/j.neucli.2007.10.008>.
- Volpe JJ. Dysmaturation of Premature Brain: Importance, Cellular Mechanisms and Potential Interventions. *Pediatr Neurol* 2019;95:42–66. <https://doi.org/10.1016/j.pediatrneurol.2019.02.016> PMID - 30975474.
- Wallois F, Routier L, Heberlé C, Mahmoudzadeh M, Bourel-Ponchel E, Moghimi S. Back to basics: the neuronal substrates and mechanisms that underlie the electroencephalogram in premature neonates. *Neurophysiol Clin* 2021;51(1):5–33. <https://doi.org/10.1016/j.neucli.2020.10.006>.
- Watanabe K, Hayakawa F, Okumura A. Neonatal EEG: a powerful tool in the assessment of brain damage in preterm infants. *Brain Dev* 1999;21(6):361–72. [https://doi.org/10.1016/S0387-7604\(99\)00034-0](https://doi.org/10.1016/S0387-7604(99)00034-0).
- Werth J, Atallah L, Andriessen P, Long X, Zwartkruis-Pelgrim E, Aarts RM. Unobtrusive sleep state measurements in preterm infants – A review. *Sleep Med Rev* 2017;32:109–22. <https://doi.org/10.1016/j.smrv.2016.03.005>.
- Whitehead K, Pressler R, Fabrizi L. Characteristics and clinical significance of delta brushes in the EEG of premature infants. *Clin Neurophysiol Pract* 2016;2:12–8. <https://doi.org/10.1016/j.cnp.2016.11.002>.